arXiv:1510.05037v1 [physics.flu-dyn] 16 Oct 2015

Transient Growth in Stochastic Burgers Flows

Diogo Poças and Bartosz Protas*
Department of Mathematics & Statistics,
McMaster University
Hamilton, Ontario L8S4K1, CANADA

October 20, 2015

Abstract

This study considers the problem of the extreme behavior exhibited by solutions to Burgers equation subject to stochastic forcing. More specifically, we are interested in the maximum growth achieved by the "enstrophy" (the Sobolev H^1 seminorm of the solution) as a function of the initial enstrophy $\mathcal{E}_0$, in particular, whether in the stochastic setting this growth is different than in the deterministic case considered by Ayala & Protas (2011). This problem is motivated by questions about the effect of noise on the possible singularity formation in hydrodynamic models. The main quantities of interest in the stochastic problem are the expected value of the enstrophy and the enstrophy of the expected value of the solution. The stochastic Burgers equation is solved numerically with a Monte Carlo sampling approach. By studying solutions obtained for a range of optimal initial data and different noise magnitudes, we reveal different solution behaviors and it is demonstrated that the two quantities always bracket the enstrophy of the deterministic solution. The key finding is that the expected values of the enstrophy exhibit the same power-law dependence on the initial enstrophy $\mathcal{E}_0$ as reported in the deterministic case. This indicates that the stochastic excitation does not increase the extreme enstrophy growth beyond what is already observed in the deterministic case.

Keywords: stochastic Burgers equation; extreme behavior; enstrophy; singularity formation; Monte Carlo

1 Introduction and Problem Statement

Many open problems related to nonlinear partial differential equations (PDEs) of mathematical physics concern the extreme behavior which can be exhibited to their solutions. By

*Corresponding author; Email bprotas@mcmaster.ca

this we mean, among other, questions concerning the maximum possible growth of certain norms of the solution of the PDE. From the physics point of view, these norms measure different properties of the solution, such as generation of small scales in the case of the Sobolev norms. The question of the maximum possible growth of solution norms is also intrinsically linked to the problem of existence of solutions to PDE problems in a given functional space. More specifically, the loss of regularity of a solution resulting from the formation of singularities usually manifests itself in an unbounded growth of some solution norms in finite time, typically referred to as "blow-up". While problems of this type remain open for many important PDEs of mathematical physics, most attention has been arguably given to establishing the regularity of the three-dimensional (3D) Navier-Stokes equations [1], a problem which has been recognized by the Clay Mathematics Institute as one of its "millennium problems" [2]. Analogous questions also remain open for the 3D inviscid Euler equation [3]. The problem we address in the present study is how the transient growth of solutions to certain nonlinear PDEs is affected by the presence of noise represented by a suitably defined stochastic forcing term in the equation. More specifically, the key question is whether via some interaction with the nonlinearity such stochastic forcing may enhance or weaken the growth of certain solution norms as compared to the deterministic case. In particular, in the case of systems exhibiting finite-time blow-up in the deterministic case it is interesting to know whether noise may accelerate or delay the formation of a singularity, or perhaps even prevent it entirely [4]. These questions are of course nuanced by the fact that they may be considered either for individual trajectories or in suitable statistical terms. We add that transient growth in linear stochastic systems is well understood [5] and here we focus on the interaction of the stochastic forcing with a particular type of nonlinearity.

Since this study is ultimately motivated by questions concerning extreme behavior in hydrodynamic models, we will focus our attention on the simplest model used in this context, namely, the one-dimensional (1D) stochastic Burgers equation defined on a periodic interval $[0, 1]$

$$\partial_t u + \frac{1}{2}\partial_x u^2 - \nu \partial_x^2 u = \zeta \qquad \text{in } (0, T] \times (0, 1), \tag{1a}$$

$$u(t, 0) = u(t, 1) \text{ and } \partial_x u(t, 0) = \partial_x u(t, 1) \qquad \text{for } t \in [0, T], \tag{1b}$$

$$u(0, x) = g(x) \qquad \text{for } x \in (0, 1), \tag{1c}$$

in which $T > 0$ represents the length of the time window of interest, $\nu > 0$ is the viscosity coefficient (hereafter we will use $\nu = 0.001$), $g \in H_p^1(0, 1)$ is the initial condition, where $H_p^1(0, 1)$ denotes the Sobolev space of periodic functions defined on $(0, 1)$ with square integrable derivatives and the norm given by [6]

$$\|u(t, \cdot)\|_{H_p^1}^2 = \int_0^1 |u(t, x)|^2 + |\partial_x u(t, x)|^2 \, dx. \tag{2}$$

For simplicity we will denote the time-space domain $D := (0, T] \times (0, 1)$ (":=" means "equal to by definition"). In equation (1a) the stochastic forcing is given by a random field $\zeta(t, x)$, $(t, x) \in D$. Therefore, at any point (t, x) our solution becomes a random variable $u =$

$u(t, x, \omega)$ for ω in some probability space Ω. We add that, while for other systems, such as e.g. the Schrödinger equation [7], one may also consider multiplicative noise, for models of the type (1a) one typically studies additive noise.

A common approach to modelling stochastic excitation in PDE systems is to describe it in terms of Gaussian white noise associated with an infinite-variance Wiener process. However, as will be discussed in Section 2 and Appendix A, such noise model does not ensure that individual solutions are well defined in the Sobolev space H^1_p and is therefore not suitable for the problem considered here. Thus, for the remainder of this paper, we shall restrict our attention to the case where ζ is the derivative of a Wiener process with finite variance, which is the most "aggressive" stochastic excitation still leaving problem (1) well-posed in H^1_p (precise definition is deferred to Section 2). We add that the stochastic Burgers equation may be regarded as a special case of the Kardar-Parisi-Zhang equation which has received some attention in the literature [8].

We now briefly summarize important results from the literature relevant to the stochastic Burgers equation. The existence and uniqueness of solutions has been proven in [9, 10] for the problem posed on the real line and in [11, 12] for a bounded domain with Dirichlet boundary conditions. In all cases, solutions can be regarded as continuous L^p-valued random processes. For the bounded domain (the case which we are interested in), convergence of numerical schemes has been established in [13] for the finite-difference approaches and in [14] for Galerkin approximations. However, in both cases only Dirichlet boundary conditions were considered. The case with the periodic boundary conditions has been recently considered in [15] for a larger class of Burgers-type equations and an abstract numerical scheme.

Given its significance in hydrodynamics [1], the key quantity of interest in our study will be the H^1 seminorm of the solution referred to as *enstrophy*

$$\mathcal{E}(u(t)) := \frac{1}{2}\int_0^1 |\partial_x u(t,x)|^2\, dx. \tag{3}$$

In the deterministic setting ($\zeta \equiv 0$ in (1a)), where Burgers equation is known to be globally well-posed [16], its solutions generically exhibit a steepening of the gradients (driven by the nonlinearity) followed by their viscous dissipation when the linear dissipative term starts to dominate. This behavior is manifested by an initial growth of enstrophy $\mathcal{E}(u(t))$, which peaks when the solution $u(t,\cdot)$ builds up the steepest front, followed by its eventual decay to zero. As a point of reference, we illustrate this generic behavior in Figure 1 in which the results were obtained by solving system (1) with $\zeta \equiv 0$, $T = 1.0$ and an "extreme" initial condition $\tilde{g}_{\mathcal{E}_0,T}$ designed to produce a maximum enstrophy growth over $[0, 1]$ for a given $\mathcal{E}_0 := \mathcal{E}(\tilde{g}_{\mathcal{E}_0,T})$ (the numerical approach used to obtain the results in Figure 1 and the construction of the extreme initial data $\tilde{g}_{\mathcal{E}_0,T}$ will be described in Sections 3 and 4, respectively). Although the evolution shown in Figure 1 corresponds to a special choice of the initial data, it is qualitatively similar to the generic case.

For deterministic systems which exhibit blow-up, singularity formation is typically signalled by unbounded growth of certain Sobolev norms [17]. This growth can often be estimated using bounds obtained with methods of functional analysis. Therefore, even for

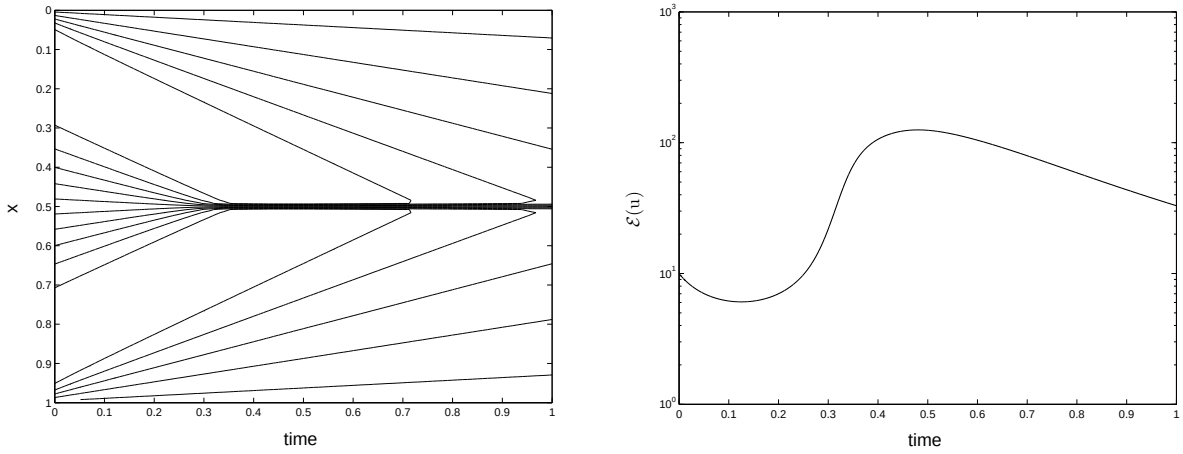

(a) (b)

Figure 1: (a) Space-time evolution of the solution $u(t,x)$ and (b) history of the enstrophy $\mathcal{E}(u(t))$ in a solution of the deterministic Burgers equation with an extreme initial condition $\tilde{g}_{\mathcal{E}_0,T}$. In figure (a) the level sets of $u(t,x)$ are plotted with increments of 0.1.

problems which are globally well-posed such as the viscous Burgers equation, it is important to understand how much the enstrophy $\mathcal{E}(u(t))$ can grow depending on the "size" of the initial data $\mathcal{E}_0 = \frac{1}{2}\int_0^1 |\partial_x g(x)|^2\, dx$, as this can provide valuable insights concerning the sharpness of the corresponding estimates. These issues are at the heart of the recently undertaken research program aiming to probe the sharpness of fundamental estimates on the growth of quadratic quantities in hydrodynamic models [18, 19, 20]. These estimates are of two types, namely, concerning the instantaneous growth (i.e., the rate of change at a fixed instant of time) and growth over finite time windows. Important progress has also been made on some related questions in the context of the 3D Navier-Stokes problem [21] which is in fact what has motivated this research program. On the other hand, to the best of our knowledge, no such estimates are available for the largest possible growth of solution norms, either instantaneously or over finite time, in the corresponding stochastic PDE models. In this area most of the research has been focused on the long-time behavior and behavior averaged with respect to time, as surveyed, e.g., in [22]. Questions concerning how noise can regularize potentially singular solutions began to be investigated relatively recently and we refer the reader to the monograph [4] for a survey of recent analytical results. Some additional results can also be found in [23, 24, 25] for the heat equation and in [26, 27] for more general systems. While most of the literature concerns analysis, one of the first computational studies of the effect of noise on singularity formation was [7] in the context of the Schrödinger equation. Among other findings, it demonstrated that the effect of the stochastic excitation depends on the precise definition of the noise in the equation.

1.1 Notation

So that we can state the questions addressed in this study in precise terms, below we introduce some useful notation. For further details the reader is referred to the monograph [28].

Probability space: we will use the triple $(\Omega, \mathcal{F}, \mathbb{P})$ to denote the probability space of interest, where Ω is a set (outcomes), $\mathcal{F}$ is a σ-algebra (events) in Ω and $\mathbb{P}$ is a probability measure on $(\Omega, \mathcal{F})$.

Random variable: if H is a Hilbert space with the norm $\|\cdot\|_H$, a function of the type $\Omega \to H$ is called an H-valued random variable; we denote by $L^2(\Omega, H)$ the space of square-integrable random variables X with the norm

$$\|X\|^2_{L^2(\Omega,H)} := \int_\Omega \|X(\omega)\|^2_H \, d\mathbb{P}(\omega) = \mathbb{E}\left[\|X\|^2_H\right].$$

Stochastic process: given a set $\mathcal{T} \subseteq \mathbb{R}$, an H-valued stochastic process is a parameterized class of H-valued random variables $\{X(t) : t \in \mathcal{T}\}$; in this paper we shall only consider two cases: either $\mathcal{T} = [0, T]$ for a stopping time T, or $\mathcal{T} = \{t_0, t_1, \ldots, t_N\}$, where $t_i \in \mathbb{R}$, $0 \le i \le N$ for some $N \in \mathbb{N}$; we observe that $\mathcal{T}$ is a compact set in both cases.

Sample path: for a given $\omega \in \Omega$, a sample path is the function $f : \mathcal{T} \to H$ defined by $f(t) = X(t, \omega)$.

Second-order continuous process: an H-valued stochastic process $X = \{X(t) : t \in \mathcal{T}\}$ is said to be second-order if $X(t) \in L^2(\Omega, H)$ for all $t \in \mathcal{T}$; it is said to be continuous if all sample paths are continuous; we denote by $\mathcal{H}_\mathcal{T}(L^2(\Omega, H))$ the space of continuous second-order H-valued processes with the norm

$$\|X\|_{\mathcal{H}_\mathcal{T}(L^2(\Omega,H))} := \sup_{t\in\mathcal{T}} \|X(t)\|_{L^2(\Omega,H)};$$

the above supremum exists because $\mathcal{T}$ is taken to be compact.

Fourier basis: the Sobolev space $H^1_p(0,1)$ introduced earlier, cf. (2), is contained in $L^2(0,1)$, which has an orthonormal basis $\{\phi_k\}_{k\in\mathbb{Z}}$; hereafter, ϕ_k will refer to elements of the Fourier basis $\phi_k(x) = e^{2\pi i k x}$, where $i := \sqrt{-1}$ is the imaginary unit; any real-valued function $u \in H^1_p$ can be written as a Fourier series

$$u(x) = \sum_{k\in\mathbb{Z}} \hat{u}_k \phi_k(x)$$

in which the Fourier coefficients $\hat{u}_k \in \mathbb{C}$ have the property $\hat{u}_k = \overline{\hat{u}}_{-k}$, where the overbar denotes complex conjugation; we can furthermore express the H^1_p norm of u in terms of its Fourier coefficients as [6]

$$\|u\|^2_{H^1_p} = \sum_{k\in\mathbb{Z}} (1 + 4\pi^2 k^2)|\hat{u}_k|^2. \tag{4}$$

Trigonometric basis: in addition to the Fourier basis introduced above, when sampling noise it will also be useful to consider the corresponding orthonormal trigonometric basis

$\{\chi_j\}_{j\in\mathbb{N}}$ with elements defined as follows

$$\begin{aligned}\chi_0(x) &= 1 = \phi_0(x),\\ \chi_{2k}(x) &= \sqrt{2}\cos(2\pi kx) = \frac{\sqrt{2}}{2}\phi_k(x) + \frac{\sqrt{2}}{2}\phi_{-k}(x),\\ \chi_{2k-1}(x) &= \sqrt{2}\sin(2\pi kx) = -i\frac{\sqrt{2}}{2}\phi_k(x) + i\frac{\sqrt{2}}{2}\phi_{-k}(x).\end{aligned}$$

Solution space: as mentioned above, a solution u to (1) at any given $(t,x) \in D$ is a random variable $u(t,x) : \Omega \to \mathbb{R}$; we will assume the solution $u = \{u(t) : 0 \le t \le T\}$ to be a continuous second-order H_p^1-valued stochastic process; in particular, this implies that $u(t) \in L^2(\Omega, H_p^1)$ for any time $t \in [0,T]$; the Fourier coefficients $\hat{u}_k = \{\hat{u}_k(t)\}_{k\in\mathbb{Z}}$ then become continuous, second-order $\mathbb{C}$-valued processes and we have the relations

$$\begin{aligned}\|u(t)\|^2_{L^2(\Omega,H_p^1)} &= \mathbb{E}\left[\sum_{k\in\mathbb{Z}}(1+4\pi^2k^2)|\hat{u}_k(t)|^2\right] = \sum_{k\in\mathbb{Z}}(1+4\pi^2k^2)\|\hat{u}_k(t)\|^2_{L^2(\Omega,\mathbb{C})},\\ \|u\|^2_{\mathcal{H}_\mathcal{T}(L^2(\Omega,H_p^1))} &= \sup_{t\in\mathcal{T}}\mathbb{E}\left[\sum_{k\in\mathbb{Z}}(1+4\pi^2k^2)|\hat{u}_k(t)|^2\right] \le \sum_{k\in\mathbb{Z}}(1+4\pi^2k^2)\|\hat{u}_k\|^2_{\mathcal{H}_\mathcal{T}(L^2(\Omega,\mathbb{C}))}.\end{aligned}$$

We will use the convention that when a given symbol appears both in the plain font and in boldface, these will represent, respectively, the function and its finite-dimensional approximation (i.e., a vector). Symbol C will denote a generic positive constant.

1.2 Summary of the Main Results

The main question we address here is how the growth of the enstrophy described by stochastic system (1), both in terms of individual trajectories and statistical properties, depends on the properties of the noise term in equation (1a), in particular, whether this growth is enhanced or weakened in comparison to the growth observed in the deterministic system [18], cf. Figure 1. We have made the following observations:

- samples of the stochastic solution tend to exhibit a larger growth of enstrophy than the deterministic solution,
- when the noise magnitude is sufficiently large relative to the initial enstrophy $\mathcal{E}_0$, the dynamics of sample solutions is entirely dominated by noise and exhibits little effect of the initial data,
- when the noise magnitude is small relative to the initial enstrophy, solution samples can be regarded as "perturbations" of the deterministic evolution with enstrophy growth dependent on $\mathcal{E}_0$,
- the enstrophy growth $\max_{t\in[0,T]}\mathcal{E}(u(t))$ in the deterministic case provides

  - an upper bound for the growth of the enstrophy of the expected value $\max_{t\in[0,T]} \mathcal{E}(\mathbb{E}[u(t)])$, and
  - a lower bound for the growth of the expected value of the enstrophy $\max_{t\in[0,T]} \mathbb{E}[\mathcal{E}(u(t))]$,
- when the noise magnitude increases proportionally to the initial enstrophy $\mathcal{E}_0$, the same growth of the expected value of the enstrophy is observed as in the deterministic case; this leads us to conclude that inclusion of stochastic forcing does not trigger any new mechanisms of enstrophy amplification.

The remainder of this paper is divided as follows: in the next section we describe our model of noise and discuss some properties of the stochastic solutions; the numerical approach is introduced in Section 3, whereas the computational results are presented and discussed in Section 4; conclusions are presented in Section 5, whereas some technical material is deferred to two appendices.

2 Structure of the Stochastic Forcing and Properties of the Solution

As is customary in the standard theory of stochastic partial differential equations (SPDEs), we write the stochastic Burgers equation (1a) in the differential form [28]

$$du = \left(\nu\partial_x^2 u - \frac{1}{2}\partial_x u^2\right)\, dt + \sigma\, dW, \tag{5}$$

where $\zeta = \sigma\frac{dW}{dt}$ in which $\sigma > 0$ is a constant and $W(t)$ is a cylindrical Wiener process. In other words, $\{W(t)\}_{t\geq 0}$ is formally given by

$$W(t) = \sum_{j\in\mathbb{N}} \gamma_j \beta_j(t)\chi_j, \tag{6}$$

where $\{\beta_j(t)\}_{j\in\mathbb{N}}$ are i.i.d standard Brownian motions and $\{\gamma_j\}_{j\in\mathbb{N}}$ are scaling coefficients. When $\forall_j\ \gamma_j = 1$, W is an infinite-variance Wiener process and ζ is Gaussian white noise. However, in this paper we focus on noise representations with ℓ^2-summable coefficients, such as

$$\gamma_0 = 1, \quad \gamma_{2k+1} = \gamma_{2k+2} = \frac{1}{k}, \qquad k > 0, \tag{7}$$

so that $W(t)$ has a *finite* variance, meaning that it is square-integrable in L^2, i.e., $W(t) \in L^2(\Omega, L^2)$, with the norm

$$\|W(t)\|^2_{L^2(\Omega,L^2)} = \sum_{j\in\mathbb{N}} |\gamma_j|^2 \|\beta_j(t)\|^2_{L^2(\Omega,\mathbb{C})} \|\chi_j\|^2_{L^2} = t\sum_{j\in\mathbb{N}} \gamma_j^2 = \left(1 + \frac{\pi^2}{3}\right) t. \tag{8}$$

For such a finite-variance Wiener process, the term ζ in equation (1a) will be referred to as the *Gaussian colored noise*.

While Gaussian white noise is commonly used in the literature on SPDEs, this choice is not, in fact, suitable for the present study. As explained in Introduction, we are interested here in the effects of stochastic excitation on the enstrophy, cf. (3), which is not defined for the Gaussian white noise, as demonstrated in Appendix A. On the other hand, Gaussian colored noise with the structure given in (6)–(8) will ensure that this quantity is well defined.

Different notions of solution of system (1) can be considered. Due to the lack of smoothness of the noise term, we do not expect to obtain solutions defined in the classical sense (i.e., solutions continuously differentiable with respect to the independent variables). One can, however, define the notion of a *mild solution* as in [11]

$$u(t) = e^{tA}g - \frac{1}{2}\int_0^t e^{(t-s)A}\partial_x u^2\, ds + \sigma \int_0^t e^{(t-s)A}\, dW(s), \tag{9}$$

where $A := \nu\partial_x^2$ is an operator acting on functions in L^2 defined such that $A\phi_k = -4\nu\pi^2k^2\phi_k$, and thus e^{tA} also acts on L^2 with

$$e^{tA}\phi_k = e^{-4\nu\pi^2k^2t}\phi_k, \qquad \phi_k \in L_2(0,1), \qquad k = 0, 1, \ldots.$$

We remark that other notions of solution also exist, for example, the notion of a *weak solution* as defined in [13]. We then have the following

Proposition 1. *For Dirichlet boundary conditions, initial condition $g \in L^2$, positive parameters ν, T, σ, Gaussian white noise and almost every $\omega \in \Omega$, there exists a unique solution u of (9). Moreover, such a solution is continuous in time and square-integrable in space, that is, $u \in C([0,T]; L^2)$.*

Proof: Theorem 3.1 in [11]. □

The present paper deviates from the results in [11] in that

- we consider a domain with periodic boundary conditions,
- we require the solutions to be squared-integrable in the stochastic sense, and
- we consider initial data $g \in H_p^1$, Gaussian colored noise defined in (6)–(8) and expect our solutions to be in the space H_p^1,

as expressed by the following Assumption.

Assumption 2. *For a given initial condition $g \in H_p^1$, positive parameters ν, T, σ and Gaussian colored noise, there exists a unique solution u of (9), which is a continuous, second-order H_p^1-valued stochastic process, that is, $u \in \mathcal{H}_{\mathcal{T}}(L^2(\Omega, H_p^1))$.*

In other words, u will be assumed to be an element in the space $\mathcal{H}_{\mathcal{T}}(L^2(\Omega, H_p^1))$ with the norm

$$\|u\|^2_{\mathcal{H}_{\mathcal{T}}(L^2(\Omega,H_p^1))} = \sup_{0\le t\le T} \|u(t)\|^2_{L^2(\Omega,H_p^1)} = \sup_{0\le t\le T} \mathbb{E}\left[\|u(t)\|^2_{H_p^1}\right].$$

3 Numerical Approach

System (1a) will be discretized with respect to three parameters, namely,

- the space variable x, using a spectral approach based on a truncated Fourier series (associated with parameter K),
- the time variable t, using a finite-difference approach based on a uniform grid in time (associated with parameter N),
- the stochastic forcing ξ, using a Monte Carlo approach to sample the noise distribution (associated with parameter S).

After fixing discretization parameters $K, N \in \mathbb{N}$, we will thus look for an approximate solution $u^{K,N}$ of the form

$$u_n^{K,N} = u^{K,N}(t_n, x) = \sum_{k=-K}^{K} \hat{u}_{k,n}^{K,N} \phi_k(x), \qquad \text{for } n = 0 \dots N. \tag{10}$$

Computation of the Fourier coefficients $\hat{u}_{k,n}^{K,N}$ will be the main purpose of the numerical approach. Each of the coefficients is a complex-valued random variable, i.e., $\hat{u}_{k,n}^{K,N} = \hat{u}_{k,n}^{K,N}(\omega)$, and information about their distribution will be provided by a Monte Carlo sampling approach. In particular, we will be interested in computing the first and second moments $\mathbb{E}[\hat{u}_{k,n}^{K,N}]$ and $\mathbb{E}[|\hat{u}_{k,n}^{K,N}|^2]$. Below we describe the different discretization steps. Although discretization in time and space is carried out with standard techniques, we provide additional details on how the stochastic aspect has been handled in these approaches. In particular, we make it precise in what sense the numerical solutions approximate the solution given in (9).

3.1 Space discretization

The stochastic process u can be described in terms of its Fourier coefficients $\hat{u}_k$, for $k \in \mathbb{Z}$. For computational purposes the expansion needs to be truncated

$$u^K = \sum_{k=-K}^{K} \hat{u}_k^K \phi_k, \tag{11}$$

where K is the spatial (spectral) discretization parameter. Since the solution u is real-valued, the Fourier coefficients satisfy the conjugate symmetry property

$$\hat{u}_{-k}^K = \overline{\hat{u}_k^K}, \qquad k = -K, \dots, K, \tag{12}$$

implying that only the ones with $k = 0, \dots, K$ need to be stored. Therefore, the discretization of the spatial domain $(0, 1)$ must consist of at least $2K + 1$ grid points and in fact, due to the need to perform dealiasing, we will use $3K$ points (rounded up to the nearest power of

two to ensure efficiency of Fast Fourier Transforms). We let $\mathbf{u}^K = [\hat{u}_k^K]$ denote the vector of Fourier coefficients in which each $\hat{u}_k^K$ is a $\mathbb{C}$-valued stochastic process. Applying the Galerkin discretization procedure we then obtain a (finite) system of stochastic ordinary differential equations (SODEs) for the Fourier coefficients

$$d\mathbf{u}^K = \left(\nu D^2\mathbf{u}^K - \frac{1}{2}D\mathbf{w}^K\right)dt + \sigma\, d\mathbf{W}^K, \tag{13}$$

where the differential operators are represented as diagonal matrices

$$\partial_x \longleftrightarrow D := \mathrm{diag}(2\pi i k, k = 0, \ldots, K), \qquad \partial_x^2 \longleftrightarrow D^2 := \mathrm{diag}(-4\pi^2 k^2, k = 0, \ldots, K), \tag{14}$$

whereas the nonlinear term u^2 is represented in terms of a convolution sum, denoted $\mathbf{w}^K = [\hat{w}_k^K]$, where

$$\hat{w}_k^K := \sum_{j\in\mathbb{Z}} \hat{u}_j^K \hat{u}_{k-j}^K = \sum_{j=m_k}^{M_k} \hat{u}_j^K \hat{u}_{k-j}^K \tag{15}$$

with $m_k := \max(-K, -K+k)$ and $M_k := \min(K, K+k)$. Rather than use the computationally expensive formula (15), the coefficients $\hat{w}_k^K$ are evaluated with a pseudospectral approach based on the Fast Fourier Transforms (FFTs) [29]. This approach involves the truncation of the nonlinear term to K Fourier coefficients and is combined with dealiasing based on the "3/2" rule [29]. The space dependence of the stochastic term in equation (1a) is also represented in terms of a truncated Fourier series

$$dW^K = \sum_{j=0}^{2K} \gamma_j d\beta_j \chi_j = \sum_{k=-K}^{K} \lambda_k d\hat{y}_k^K \phi_k, \tag{16}$$

so that $d\mathbf{W}^K = [d\hat{y}_k^K]$, where $\hat{y}_k^K$ are $\mathbb{C}$-valued stochastic processes obtained by converting representation (6) from the trigonometric basis to the Fourier basis, i.e.,

$$\begin{aligned}
&\hat{y}_0^K = \beta_0(t_n),\\
&\hat{y}_k^K = \frac{\sqrt{2}}{2}\beta_{2k}(t_n) - i\frac{\sqrt{2}}{2}\beta_{2k-1}(t_n), \qquad \hat{y}_{-k}^K = \overline{\hat{y}_k^K}, \qquad k = 1, \ldots, K.
\end{aligned}$$

The scaling coefficients λ_k in (16) are determined by the coefficients γ_j, defined in (7), so that

$$\lambda_0 = \gamma_0 = 1, \quad \lambda_k = \lambda_{-k} = \gamma_{2k} = \gamma_{2k-1} = \frac{1}{k}, \qquad k > 0. \tag{17}$$

Finally, we also discretize the initial condition $u(0, x) = g(x)$

$$u^K(0) = g^K = \sum_{k=-K}^{K} \hat{g}_k \phi_k \tag{18}$$

with $\mathbf{g}^K = [\hat{g}_k]$ the corresponding vector of the Fourier coefficients. For a fixed $K \in \mathbb{N}$, system (13) consists of $(K+1)$ $\mathbb{C}$-valued SODEs which are to be interpreted in terms of Itô's integral form

$$\mathbf{u}^K(t) = \mathbf{g}^K + \int_0^t \left(\nu D^2 \mathbf{u}^K(s) - \frac{1}{2} D\mathbf{w}^K(s)\right) ds + \int_0^t \sigma \, d\mathbf{W}^K(s). \tag{19}$$

In the literature there exist rigorous results concerning the convergence of numerical approximations to the stochastic Burgers equation — for example, in [13] this was proved for a finite-difference technique applied to a problem subject to the Dirichlet boundary conditions and stochastic excitation with Gaussian white noise, whereas in [14] a similar result was proved for a Galerkin technique. Since obtaining an analogous result for the present problem is outside the scope of this study, we will leave it as the following assumption.

Assumption 3. *For a given initial condition $g \in H_p^1$, positive parameters ν, T, σ, Gaussian colored noise, and for each $K \in \mathbb{N}$, system (19) admits a unique solution $\mathbf{u}^K$, which is a vector of continuous, second order $\mathbb{C}$-valued stochastic processes. Moreover, u^K converges to the solution u of (9) in the H_p^1-norm, in the sense that*

$$\|u - u^K\|_{\mathcal{H}_\mathcal{T}(L^2(\Omega, H_p^1))} \underset{K\to\infty}{\longrightarrow} 0;$$

furthermore, there is a constant $\alpha > 0$ such that we have a bound of the form

$$\|u(t) - u^K(t)\|_{L^2(\Omega, H_p^1)} \leq CK^{-\alpha} \text{ for all } 0 \leq t \leq T$$

for a constant C depending on g, ν, T and σ.

3.2 Time discretization

We are interested in computing the approximate solution u^K at equispaced discrete time levels. We let N denote the number of time levels given by $t_n = n\Delta t$, where $n = 0, \ldots, N$ and $\Delta t := \frac{T}{N}$. Then, we have

$$u_n^{K,N} := u^K(t_n) = \sum_{k=-K}^{K} \hat{u}_{k,n}^{K,N} \phi_k, \tag{20}$$

where each coefficient $\hat{u}_{k,n}^{K,N} := \hat{u}_k^K(t_n)$ is a $\mathbb{C}$-valued random variable. Each $u_n^{K,N}$ is an H_p^1-valued random variable, so that $\{u_n^{K,N} : n = 0, \ldots, N\}$ forms an H_p^1-valued discrete stochastic process. We can also define $\mathbf{u}_n^{K,N} = \left[\hat{u}_{k,n}^{K,N}\right]$ as the corresponding vector of Fourier coefficients. The approximate solution is then obtained via a semi-implicit Euler method, defined as

$$\mathbf{u}_{n+1}^{K,N} = \mathbf{u}_n^{K,N} + \left(\nu D^2 \mathbf{u}_{n+1}^{K,N} - \frac{1}{2} D\mathbf{w}_n^{K,N}\right) \Delta t + \sigma \Delta \mathbf{W}_n^{K,N}, \quad n = 0, \ldots, N-1, \tag{21}$$

in which the dissipative term is treated implicitly whereas the nonlinear and the stochastic terms are treated explicitly. Some remarks are in order. First of all, $u_n^{K,N}$ is square-integrable with respect to the probability measure if and only if $\hat{u}_{k,n}^{K,N}$ is square-integrable for every k, with the equality

$$\|u_n^{K,N}\|^2_{L^2(\Omega,H_p^1)} = \sum_{k=-K}^{K} (1+4\pi^2k^2)\|\hat{u}_{k,n}^{K,N}\|^2_{L^2(\Omega,\mathbb{C})}.$$

Next, we discuss the noise term (or, to be precise, the noise matrix) $\Delta\mathbf{W}_n^{K,N} = [\lambda_k \Delta\hat{y}_{k,n}^{K,N}]$. Let $\Delta\beta_j(t_n) := \beta_j(t_{n+1}) - \beta_j(t_n)$ denote the n-th increment associated to the Brownian motion β_j. Then, the increments are independent and with a Gaussian distribution $\{\Delta\beta_j(t_n)\} \overset{\text{iid}}{\sim} \mathcal{N}(0,\Delta t)$. By transforming from the trigonometric basis to the Fourier basis, we can re-express the noise term as

$$\Delta W_n^{K,N} = \sum_{j=0}^{2K} \gamma_j \Delta\beta_j(t_n)\chi_j = \sum_{k=-K}^{K} \lambda_k \Delta\hat{y}_{k,n}^{K,N}\phi_k, \tag{22}$$

so that $\Delta\hat{y}_{k,n}^{K,N}$ are complex-valued random variables given by

$$\begin{aligned}
&\Delta\hat{y}_{0,n}^{K,N} = \Delta\beta_0(t_n),\\
&\Delta\hat{y}_{k,n}^{K,N} = \frac{\sqrt{2}}{2}\Delta\beta_{2k}(t_n) - i\frac{\sqrt{2}}{2}\Delta\beta_{2k-1}(t_n), \quad \Delta\hat{y}_{-k,n}^{K,N} = \overline{\Delta\hat{y}_{k,n}^{K,N}}, \qquad k=1,\dots,K.
\end{aligned}$$

In particular, we note that $\|\Delta\hat{y}_{k,n}^{K,N}\|^2_{L^2(\Omega,\mathbb{C})} = \Delta t$ for any k and n. Given that D^2 and D are diagonal matrices, cf. (14), we obtain the following recursive expression for the Fourier coefficients at the different time levels

$$\hat{u}_{k,n+1}^{K,N} = \frac{1}{1+4\nu\pi^2k^2\Delta t}\left(\hat{u}_{k,n}^{K,N} - \pi i\Delta t k\hat{w}_{k,n}^{K,N} + \sigma\lambda_k\Delta\hat{y}_{k,n}^{K,N}\right), \quad k=0,\dots,N, \tag{23a}$$

$$\hat{u}_{k,0}^{K,N} = \hat{g}_k, \qquad n=0,1,\dots. \tag{23b}$$

Finally, we discuss the convergence of the method with respect to temporal discretization. For any discretization parameters K, N, it is clear from (23) that the $\mathbb{C}$-valued random variables $\hat{u}_{k,n}^{K,N}$ are well-defined and square-integrable for any $k = -K,\dots,K$ and $n = 0,\dots,N$, so that $u^{K,N}$ is a discrete second-order H_p^1-valued stochastic process. One way to show convergence to the true solution of (9) would be to prove that, for any fixed space discretization described by parameter K, we have convergence with the increase of N. We therefore formulate the following assumption.

Assumption 4. *For the given initial condition $g \in H_p^1$, problem parameters ν, T, σ, and any large enough space discretization parameter K, the discrete stochastic process $\mathbf{u}^{K,N}$ solving* (21)*, i.e., with components defined by* (23)*, converges to the continuous stochastic process $\mathbf{u}^K$ which solves* (19)*, in the sense that*

$$\|u^K(T) - u_N^{K,N}\|_{L^2(\Omega,H_p^1)} \underset{N\to\infty}{\longrightarrow} 0;$$

moreover, there is a constant $\beta > 0$ such that we have a bound of the form

$$\|u^K(t_n) - u_n^{K,N}\|_{L^2(\Omega,H_p^1)} \leq CN^{-\beta},$$

for a constant C depending on g, ν, T and σ (in particular, C does not depend on K).

Based on this assumption, we can now make the following assertion.

Lemma 5. *Under Assumptions 3 and 4, the discrete stochastic process $u^{K,N}$ solving* (21) *converges to the continuous stochastic process u which solves* (9)*, in the sense that*

$$\|u(T) - u_N^{K,N}\|_{L^2(\Omega,H_p^1)} \underset{K,N\to\infty}{\longrightarrow} 0;$$

moreover, there are constants $\alpha, \beta > 0$ such that we have a bound of the form

$$\|u(t_n) - u_n^{K,N}\|_{L^2(\Omega,H_p^1)} \leq C\left(K^{-\alpha} + N^{-\beta}\right) \quad \textit{for all } n = 0, \ldots, N,$$

for a constant C depending on g, ν, T and σ.

Proof. The claim follows immediately from Assumptions 3 and 4 and the triangle inequality

$$\|u(t_n) - u_n^{K,N}\|_{L^2(\Omega,H_p^1)} \leq \|u(t_n) - u^K(t_n)\|_{L^2(\Omega,H_p^1)} + \|u^K(t_n) - u_n^{K,N}\|_{L^2(\Omega,H_p^1)}.$$

□

3.2.1 Noise Variance

We briefly comment on the noise term $\Delta W_n^{K,N}$ appearing in (22), where $W_n^{K,N}$ denotes an approximation of a finite-variance Wiener process. We can compute its variance using the fact that $\|\Delta\hat{y}_{k,n}^{K,N}\|_{L^2(\Omega,\mathbb{C})}^2 = \Delta t$, so that we obtain

$$\mathbb{V}[\sigma\Delta W_n^{K,N}] = \sigma^2\|\Delta W_n^{K,N}\|_{L^2(\Omega,H_p^1)}^2 = \sigma^2\sum_{k=-K}^{K}\lambda_k^2\|\Delta\hat{y}_{k,n}^{K,N}\|_{L^2(\Omega,\mathbb{C})}^2 = \sigma^2\Delta t\left(1 + 2\sum_{k=1}^{K}\frac{1}{k^2}\right). \tag{24}$$

We now recall that in our model the space-time noise term is given as $\zeta = \sigma\frac{dW}{dt}$. Discretizing this formula, we obtain $\zeta_n^{K,N} = \sigma\frac{\Delta W_n^{K,N}}{\Delta t}$, so that

$$\mathbb{V}[\zeta_n^{K,N}] = \sigma^2\frac{\left(1 + 2\sum_{k=1}^{K}\frac{1}{k^2}\right)}{\Delta t} = \frac{1}{T}\sigma^2 N\left(1 + 2\sum_{k=1}^{K}\frac{1}{k^2}\right) \underset{K\to\infty}{\longrightarrow} \frac{1+\pi^2/3}{T}\sigma^2 N. \tag{25}$$

Evidently, if σ is constant, the noise variance grows without bound as we increase the time discretization parameter N (but remains bounded with respect to the increase of the space discretization parameter K). Thus, even though the Wiener process W has finite variance, its derivative is a model for *infinite-variance colored noise*.

3.3 Stochastic Sampling

In the previous subsections we presented a method to compute a particular instance of the stochastic solution corresponding to a given noise sample $\Delta W^{K,N}$ (given by a set of sampled coefficients $[\Delta\hat{y}_{k,n}^{K,N}]$). In the Monte Carlo approach we repeat the process described in (23) for a sequence of noise samples $\Delta W_1^{K,N,S}, \ldots, \Delta W_S^{K,N,S}$, where S is a *sampling discretization parameter*, thus obtaining a sequence of solution samples $u_1^{K,N,S}, \ldots, u_S^{K,N,S}$. We recall that the quantity of interest that we wish to compute is the enstrophy of the solution defined in (3). For an approximate solution $u^{K,N}$ the enstrophy can be directly computed from its Fourier coefficients,

$$\mathcal{E}(u_n^{K,N}) = \frac{1}{2}\sum_{k=-K}^{K} 4\pi^2 k^2 |\hat{u}_{k,n}^{K,N}|^2 = \sum_{k=1}^{K} 4\pi^2 k^2 |\hat{u}_{k,n}^{K,N}|^2, \qquad n = 0, \ldots, N. \tag{26}$$

However, in the stochastic setting, there are two distinct quantities of interest corresponding to (3) and (26): one can either consider the *enstrophy of the expected value* of the solution, i.e.,

$$\mathcal{E}(\mathbb{E}[u_n^{K,N}]) = \sum_{k=1}^{K} 4\pi^2 k^2 |\mathbb{E}[\hat{u}_{k,n}^{K,N}]|^2, \qquad n = 0, \ldots, N, \tag{27}$$

or the *expected value of the enstrophy* of the solution, i.e.,

$$\mathbb{E}[\mathcal{E}(u_n^{K,N})] = \sum_{k=1}^{K} 4\pi^2 k^2 \mathbb{E}[|\hat{u}_{k,n}^{K,N}|^2], \qquad , n = 0, \ldots, N. \tag{28}$$

Estimates of both these quantities can be obtained using the *average* estimator [28, Section 4.4]

$$\mathcal{E}(\mathbb{E}[u_n^{K,N}]) \approx \sum_{k=1}^{K} 4\pi^2 k^2 \left| \frac{1}{S}\sum_{s=1}^{S} \hat{u}_{k,n,s}^{K,N,S} \right|^2, \tag{29a}$$

$$\mathbb{E}[\mathcal{E}(u_n^{K,N})] \approx \sum_{k=1}^{K} 4\pi^2 k^2 \frac{1}{S}\sum_{s=1}^{S} \left| \hat{u}_{k,n,s}^{K,N,S} \right|^2. \tag{29b}$$

We observe that in (29a)–(29b) we use averages to estimate the expected value and the second moment of the Fourier coefficients $\hat{u}_{k,n,s}^{K,N,S}$, which can be expressed as

$$\mathbb{E}[\hat{u}_{k,n}^{K,N}] \approx \hat{u}_{k,n}^{K,N,S} := \frac{1}{S}\sum_{s=1}^{S} \hat{u}_{k,n,s}^{K,N,S}, \tag{30}$$

$$\mathbb{E}[|\hat{u}_{k,n}^{K,N}|^2] \approx \hat{w}_{k,n}^{K,N,S} := \frac{1}{S}\sum_{s=1}^{S} \left| \hat{u}_{k,n,s}^{K,N,S} \right|^2. \tag{31}$$

The two quantities in (27)–(28) are related via Jensen's inequality [28]

$$\mathcal{E}(\mathbb{E}[u_n^{K,N}]) \;\leq\; \mathbb{E}[\mathcal{E}(u_n^{K,N})]. \tag{32}$$

We now discuss the convergence of the method with respect to the number of samples, in particular, the convergence of the average solution to the expected value. It is clear from (30) and our previous discussion that, for any discretization parameters K, N and S, the $\mathbb{C}$-valued random variables $\hat{u}_{k,n}^{K,N,S}$ are well-defined and square-integrable, so that

$$u_n^{K,N,S} = \sum_{k=1}^{K} \hat{u}_{k,n}^{K,N,S}\phi_k, \qquad \mathbf{u}_n^{K,N,S} = \left[\hat{u}_{k,n}^{K,N,S}\right] \tag{33}$$

define a discrete second-order H_p^1-valued stochastic process $u^{K,N,S}$. We can then use standard tools of probability to show the convergence of the estimators $u_n^{K,N,S}$ to the corresponding expected values, as made precise by the following assertions.

Lemma 6. *The discrete stochastic process $u^{K,N,S}$ defined in* (33) *converges to the expected value $\mathbb{E}\left[u^{K,N}\right]$, where $u^{K,N}$ is the discrete stochastic process solving* (21)*, in the sense that*

$$\left\|\mathbb{E}\left[u_n^{K,N}\right] - u_n^{K,N,S}\right\|_{L^2(\Omega,H_p^1)} \underset{S\to\infty}{\longrightarrow} 0 \quad \textit{for all } n = 0,\dots,N;$$

moreover, we have a bound of the form

$$\left\|\mathbb{E}\left[u_n^{K,N}\right] - u_n^{K,N,S}\right\|_{L^2(\Omega,H_p^1)} \leq CS^{-1/2},$$

for a constant $C = \left\|\mathbb{E}\left[u_n^{K,N}\right] - u_n^{K,N}\right\|_{L^2(\Omega,H_p^1)}$.

Proof. To streamline the exposition, the proof can be found in the Appendix. □

Theorem 7. *Under Assumptions 3 and 4, the discrete stochastic process $u^{K,N,S}$ defined in* (33) *converges to the expected value $\mathbb{E}[u]$, where u is the continuous stochastic process that solves* (5)*, in the sense that*

$$\left\|\mathbb{E}[u(T)] - u_N^{K,N,S}\right\|_{L^2(\Omega,H_p^1)} \underset{K,N,S\to\infty}{\longrightarrow} 0;$$

moreover, there are constants $\alpha, \beta > 0$ such that we have a bound of the form

$$\left\|\mathbb{E}[u(t_n)] - u_n^{K,N,S]}\right\|_{L^2(\Omega,H_p^1)} \leq C\left(K^{-\alpha} + N^{-\beta} + S^{-1/2}\right) \qquad \textit{for all } n = 0,\dots,N,$$

for a constant C depending on g, ν, T and σ.

Proof. The claim follows from the triangle inequality

$$\left\|\mathbb{E}[u(t_n)] - u_n^{K,N,S}\right\|_{L^2(\Omega,H_p^1)} \leq \left\|\mathbb{E}[u(t_n)] - \mathbb{E}[u_n^{K,N}]\right\|_{L^2(\Omega,H_p^1)} + \left\|\mathbb{E}[u_n^{K,N}] - u_n^{K,N,S}\right\|_{L^2(\Omega,H_p^1)},$$

Jensen's inequality

$$\left\|\mathbb{E}[u(t_n)] - \mathbb{E}[u_n^{K,N}]\right\|_{L^2(\Omega,H_p^1)} = \left\|\mathbb{E}[u(t_n) - u_n^{K,N}]\right\|_{H_p^1} \leq \left\|u(t_n) - u_n^{K,N}\right\|_{L^2(\Omega,H_p^1)},$$

and Lemmas 5 and 6. □

Theorem 8. *Under Assumptions 3 and 4, the discrete stochastic process $u^{K,N,S}$ defined in* (33) *converges in probability to the expected value $\mathbb{E}[u]$, where u is the continuous stochastic process that solves* (5)*, in the sense that*

$$\mathbb{P}\left(\left\|\mathbb{E}[u(T)] - u_N^{K,N,S}\right\|_{H_p^1} \geq \epsilon\right) \underset{K,N,S\to\infty}{\longrightarrow} 0,$$

valid for all $\epsilon > 0$; moreover, there are constants $\alpha, \beta > 0$ such that we have a bound of the form

$$\mathbb{P}\left(\left\|\mathbb{E}[u(T)] - u_N^{K,N,S}\right\|_{H_p^1} \geq \epsilon\right) \leq \frac{C}{\epsilon^2}\left(K^{-2\alpha} + N^{-2\beta} + S^{-1}\right), \qquad \text{for all } n = 0, \ldots, N,$$

valid for all $\epsilon > 0$ and for a constant C depending on g, ν, T and σ.

Proof. Using Chebyshev's inequality, we obtain

$$\begin{aligned}
\mathbb{P}\left(\left\|\mathbb{E}[u(T)] - u_N^{K,N,S}\right\|_{H_p^1} \geq \epsilon\right) &\leq \frac{1}{\epsilon^2}\int_{\left\{\left\|\mathbb{E}[u(T)]-u_N^{K,N,S}\right\|_{H_p^1}\geq\epsilon\right\}} \left\|\mathbb{E}[u(T)] - u_N^{K,N,S}\right\|_{H_p^1}^2 d\mathbb{P}(\omega) \\
&\leq \frac{1}{\epsilon^2}\int_{\Omega} \left\|\mathbb{E}[u(T)] - u_N^{K,N,S}\right\|_{H_p^1}^2 d\mathbb{P}(\omega) \\
&= \frac{1}{\epsilon^2}\left\|\mathbb{E}[u(T)] - u_N^{K,N,S}\right\|_{L^2(\Omega,H_p^1)}^2 \\
&\leq \frac{C}{\epsilon^2}(K^{-2\alpha} + N^{-2\beta} + S^{-1}),
\end{aligned}$$

where the last step follows from Theorem 7. □

4 Computational Results

In this section we use the numerical approach introduced above to study the effect of the stochastic excitation with the structure described in Section 2 on the enstrophy growth in the solutions of Burgers equation. More specifically, we will address the question formulated in Introduction, namely, whether or nor the presence of noise can further amplify the maximum growth of enstrophy characterized in the deterministic setting in [18]. We will do so by studying how the growth of the two quantities, $\mathcal{E}(\mathbb{E}[u_n^{K,N}])$ and $\mathbb{E}(\mathcal{E}[u_n^{K,N}])$ introduced in Section 3.3, is affected by the stochastic excitation as a function of the initial enstrophy $\mathcal{E}_0 = \frac{1}{2}\int_0^1 |\partial_x g(x)|^2\, dx$. Unless indicated otherwise, we will consider a time interval of length $T = 1$ and will solve system (1) subject to *optimal* initial condition $\tilde{g}_{\mathcal{E}_0,T}$ which is designed to produce the largest possible growth of enstrophy at time T for all initial data in H_p^1 with enstrophy $\mathcal{E}_0$. The procedure for obtaining such optimal initial data is discussed in [18] and the optimal initial conditions corresponding to $\mathcal{E}_0 = 10$ and different time windows T are

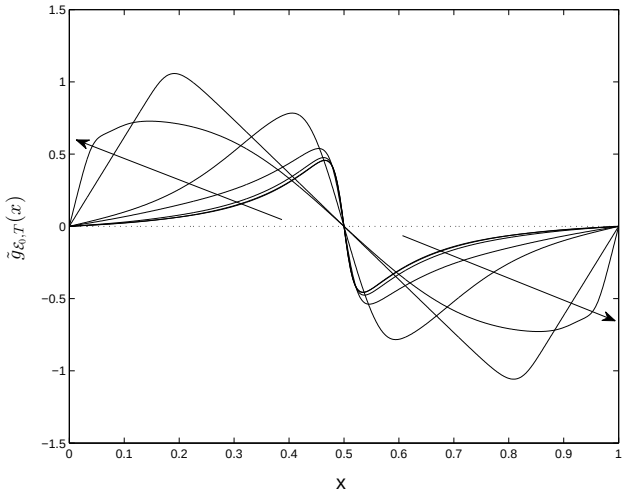

Figure 2: Optimal initial conditions $\tilde{g}_{\mathcal{E}_0,T}(x)$ for $\mathcal{E}_0 = 10$ and T ranging from 10^{-3} to 1 [18] (arrows indicate the directions of increase of T).

shown in Figure 2. We see in this figure that, as T increases, the form of the optimal initial data changes from a "shock wave" to a "rarefaction wave".

In our numerical solution of the stochastic Burgers equation, cf. (23), we used the following values of the discretization parameters: $K = 341 = \lfloor \frac{1024}{3} \rfloor$ dealiased complex Fourier modes (corresponding to $M = 1024$ grid points in the physical space), $N = 20,000$ time steps and $S = 1000$ Monte Carlo samples. The convergence of our numerical procedure was verified and the indicated values of the numerical parameters represent a reasonable trade-off between accuracy and the computational cost. In the subsections below we first recall some properties of the extreme enstrophy growth in the deterministic setting and then discuss the effect of the noise on the enstrophy growth over time and globally as a function of $\mathcal{E}_0$.

4.1 Deterministic Case Revisited

The deterministic case will serve as a reference and here we summarize some key facts about the corresponding maximum enstrophy growth. The reader is referred to studies [21, 18, 30, 31] for additional details. As illustrated in Figure 1, a typical behavior of the solutions to Burgers equation involves a steepening of the initial gradients, which is manifested as a growth of enstrophy, followed by their dissipation when the enstrophy eventually decreases. The key question is how the enstrophy at some fixed time $\mathcal{E}(T)$, or the maximum enstrophy $\max_{t\in[0,T]} \mathcal{E}(t)$, depend on the initial enstrophy $\mathcal{E}_0$. While the sharpest available analytical estimate predicts $\max_{t\geq 0} \mathcal{E}(t) \leq C\,\mathcal{E}_0^3$ for large $\mathcal{E}_0$, it was found in [18] that under the most extreme circumstances the actual system evolution does not saturate this upper bound producing instead $\max_{t\in[0,T]} \mathcal{E}(t) \sim \mathcal{E}_0^{3/2}$. These results are illustrated in Figure 3a,b, where we can also see that for very short evolution times growth only linear in $\mathcal{E}_0$ is observed (this is because for small $\mathcal{E}_0$ the solutions do not have enough time to produce sharp gradients). Since for increasing $\mathcal{E}_0$ the maximum growth of enstrophy is achieved for different T, the

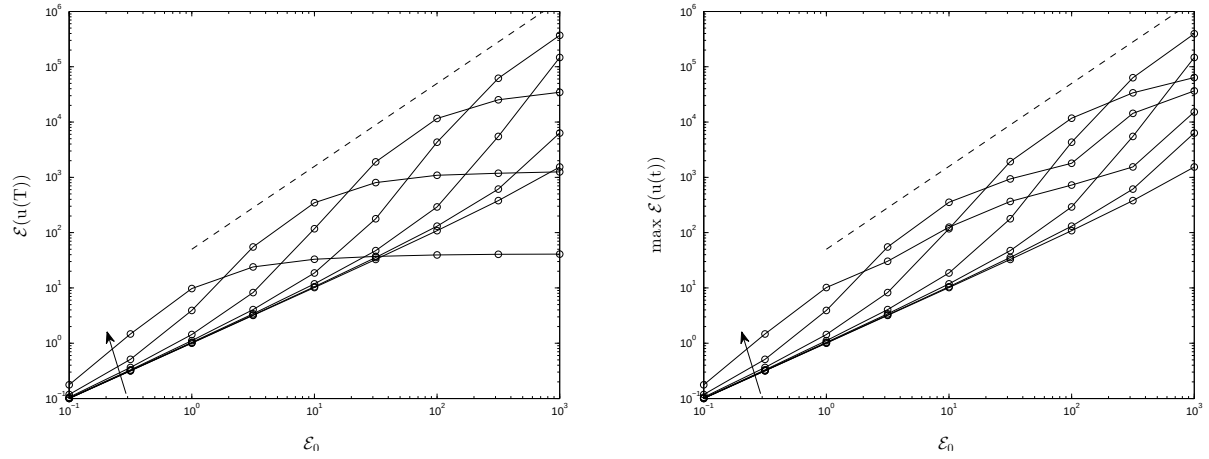

(a) (b)

Figure 3: Dependence of (a) the enstrophy $\mathcal{E}(T)$ at a final time T and (b) the maximum enstrophy $\max_{t\in[0,T]} \mathcal{E}(t)$ on the initial enstrophy $\mathcal{E}_0$ for the optimal initial data $\tilde{g}_{\mathcal{E}_0,T}$ with T in the range from 10^{-3} to 1. Arrows indicate the direction of increasing T and the dashed lines correspond to the power law $C\,\mathcal{E}_0^{3/2}$.

power-law behavior is obtained by taking a maximum of $\mathcal{E}(T)$ or $\max_{t\in[0,T]} \mathcal{E}(t)$ with respect to T (represented in Figures 3a,b as "envelopes" of the curves corresponding to different values of T).

4.2 Effect of Noise on Time Evolution

We now analyze the effect of noise, both in terms of individual trajectories and in the statistical sense, as a function of time during the evolution starting from the optimal initial data $\tilde{g}_{\mathcal{E}_0,T}$ with fixed initial enstrophy $\mathcal{E}_0 = 10$. Stochastic solutions corresponding to "small" noise magnitude $\sigma^2 = 10^{-2}$ and "large" noise magnitude $\sigma^2 = 1$ are illustrated in Figures 4 and 5, respectively. The individual stochastic trajectories are shown as functions of space and time in Figures 4a and 5a. We see that in the small-noise case the effect of the stochastic excitation is to gradually change the position of the "shock wave" (cf. Figures 1a and 4a). In the large-noise case the steep gradient region from the initial data is gone and is replaced with spontaneously appearing and interacting shocks which move in a largely structureless field (Figure 5a). The corresponding evolutions of the enstrophy of some sample stochastic solutions $\mathcal{E}(u_s^{K,N,S}(t))$, $s = 1, 2$, the expected value of the enstrophy $\mathbb{E}(\mathcal{E}[u^{K,N}(t)])$ and the enstrophy of the expected value of the solution $\mathcal{E}(\mathbb{E}[u^{K,N}(t)])$ are shown in Figures 4b and 5b for the two noise levels where they are also compared to the enstrophy evolution $\mathcal{E}(t)$ in the deterministic case. We see that the enstrophy of the sample stochastic solutions tends to exceed the enstrophy of the deterministic solution for most, albeit not all, times. As regards the relation of the the expected value of the enstrophy $\mathbb{E}(\mathcal{E}[u^{K,N}(t)])$ and the enstrophy of the expected value of the solution $\mathcal{E}(\mathbb{E}[u^{K,N}(t)])$ to the enstrophy $\mathcal{E}(t)$ in the deterministic

case, the following relationship is observed

$$\mathcal{E}(\mathbb{E}[u^{K,N}(t)]) \;\leq\; \mathcal{E}(t) \;\leq\; \mathbb{E}[\mathcal{E}(u^{K,N}(t))], \quad t > 0 \tag{34}$$

for both noise levels. While the relation between $\mathcal{E}(\mathbb{E}[u^{K,N}(t)])$ and $\mathbb{E}[\mathcal{E}(u^{K,N}(t))]$ is a consequence of Jensen's inequality (32), the fact that these two quantities in fact bracket the enstrophy of the deterministic solution uniformly in time appears rather non-obvious. This conclusion is further elaborated in Figure 6 where we show the time evolution of the three quantities from (34) for increasing noise levels. We see that the difference between $\mathcal{E}(\mathbb{E}[u^{K,N}(t)])$ and $\mathbb{E}[\mathcal{E}(u^{K,N}(t))]$ increases with the noise magnitude σ^2, such that at large noise levels the enstrophy of the expected value of the solution exhibits no growth at all. The fluctuations evident in $\mathcal{E}(\mathbb{E}[u^{K,N}(t)])$ corresponding to the largest noise level are a numerical artefact resulting from an insufficient number of Monte Carlo samples. This is due to the fact that increased noise levels slow down the convergence of the Monte Carlo approach, a phenomenon which may in principle be deduced from Theorems 7 and 8 by noting the possible dependence of the constant C on the noise magnitude σ^2.

4.3 Global Effect of Noise on Enstrophy Growth for Varying $\mathcal{E}_0$

In this section we analyze how the diagnostic quantities

$$\mathbb{E}(\mathcal{E}[u^{K,N}(T)]), \qquad \mathcal{E}(\mathbb{E}[u^{K,N}(T)]), \tag{35a}$$

$$\max_{t\in[0,T]} \mathbb{E}(\mathcal{E}[u^{K,N}(t)]), \qquad \max_{t\in[0,T]} \mathcal{E}(\mathbb{E}[u^{K,N}(t)]) \tag{35b}$$

for some given T depend on the initial enstrophy $\mathcal{E}_0$ and whether the presence of the stochastic excitation modifies the power-law dependence of the quantities (35b) on $\mathcal{E}_0$ as compared to the deterministic case (cf. Section 4.1). We will do this in two cases, namely, when for different values of the initial enstrophy $\mathcal{E}_0$ the noise level σ^2 is fixed and when it is proportional to $\mathcal{E}_0$. In regard to the first case, in Figures 7a and 7b we show the dependence of the quantities (35a) and (35b) with $T = 1.0$ on $\mathcal{E}_0$ for different fixed noise levels. The quantities $\mathcal{E}(\mathbb{E}[u^{K,N}(T)])$ and $\mathbb{E}[\mathcal{E}(u^{K,N}(T))]$ for different time horizons T are plotted as functions of $\mathcal{E}_0$ for small and large noise levels, respectively, in Figures 8 and 9. These plots are therefore the stochastic counterparts of Figure 3 representing the deterministic case [18]. We see that with a fixed T both $\mathcal{E}(\mathbb{E}[u^{K,N}(T)])$ and $\mathbb{E}[\mathcal{E}(u^{K,N}(T))]$ saturate at a level depending on the noise magnitude σ^2 (Figure 7a). Analogous behavior is observed for a fixed noise level and increasing time intervals in Figures 8 and 9, from which we can also conclude that when we maximize the quantities $\mathcal{E}(\mathbb{E}[u^{K,N}(T)])$ and $\mathbb{E}[\mathcal{E}(u^{K,N}(T))]$ over all considered values of T, then the resulting quantity will scale proportionally to $\mathcal{E}_0^{3/2}$, which is the same behavior as observed in the deterministic case (Figure 3). The process of maximizing with respect to T is represented schematically in Figures 8 and 9 as "envelopes" of the curves corresponding to different values of T. As regards the behavior of the quantities (35b), for every noise level we observe a transition from a noise-dominated behavior, where $\max_{t\in[0,T]} \mathbb{E}(\mathcal{E}[u^{K,N}(t)])$ does not increase with $\mathcal{E}_0$ when $\mathcal{E}_0$ is small, to a nonlinearity-dominated regime in which $\max_{t\in[0,T]} \mathbb{E}(\mathcal{E}[u^{K,N}(t)])$ grows with $\mathcal{E}_0$ (Figure 7b). As regards

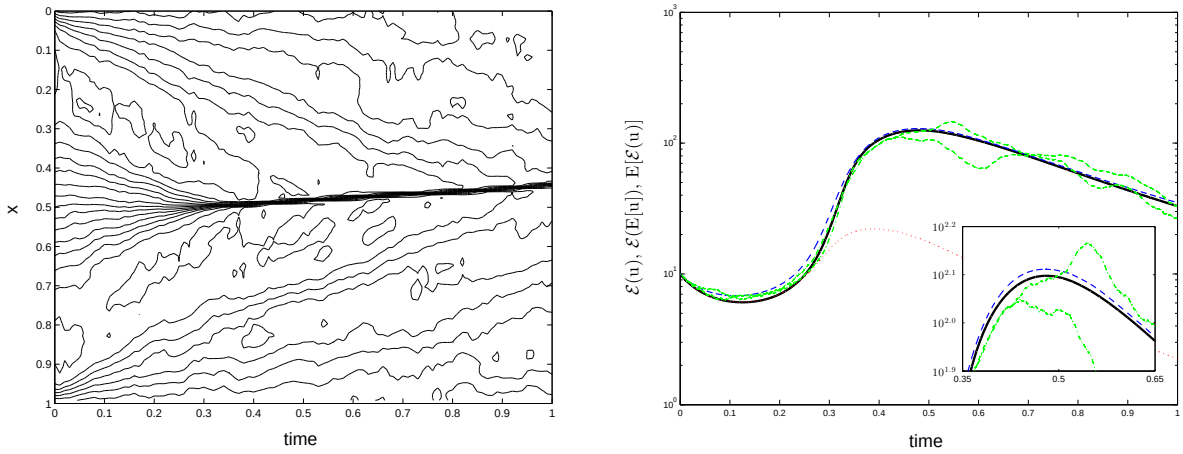

(a) (b)

Figure 4: [Small noise case: $\sigma^2 = 10^{-2}$] (a) Sample stochastic solution $u^{K,N,S}(t,x)$ as a function of space and time (the level sets are plotted with the increments of 0.1), (b) evolution of enstrophy of two sample stochastic solutions $\mathcal{E}(u_s^{K,N,S}(t))$, $s = 1, 2$, (green dash-dotted lines), the enstrophy of the deterministic solution $\mathcal{E}(u(t))$ (black solid line), the expected value of the enstrophy $\mathbb{E}(\mathcal{E}[u^{K,N}(t)])$ (blue dashed line) and the enstrophy of the expected value of the solution $\mathcal{E}(\mathbb{E}[u^{K,N}(t)])$ (red dotted line). The initial data used was $\tilde{g}_{\mathcal{E}_0,T}$ with $\mathcal{E}_0 = 10$ and $T = 1$. The inset in figure (b) shows details of the evolution during the subinterval $[0.35, 0.65]$.

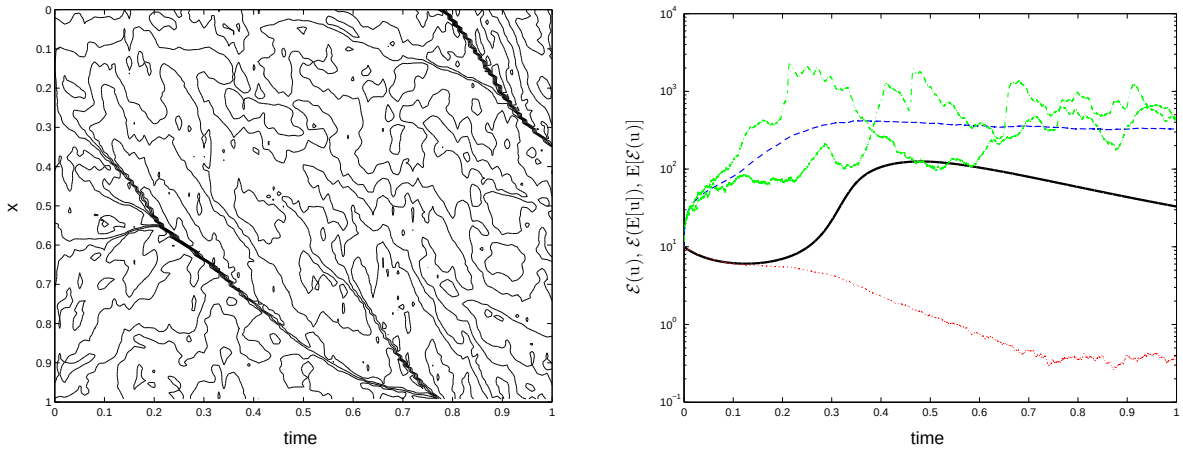

(c) (d)

Figure 5: [Large noise case: $\sigma^2 = 1$] (see previous figure for details).

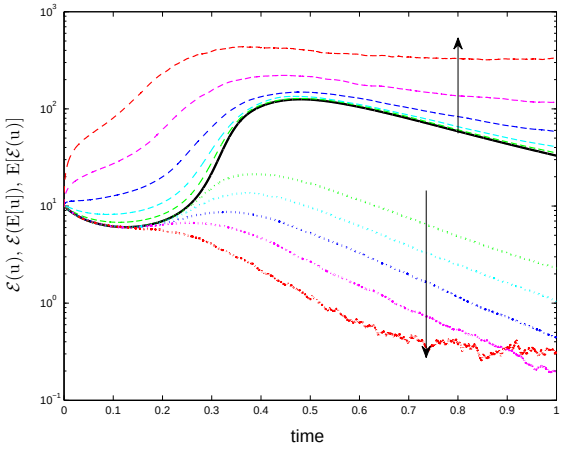

Figure 6: The expected value of the enstrophy $\mathbb{E}(\mathcal{E}[u^{K,N}(t)])$ (dashed lines), the enstrophy of the expected value of the solution $\mathcal{E}(\mathbb{E}[u^{K,N}(t)])$ (dotted lines) and the enstrophy $\mathcal{E}(t)$ of the deterministic solution (thick solid line) as functions of time for the initial condition $\tilde{g}_{\mathcal{E}_0,T}$ with $\mathcal{E}_0 = 10$, $T = 1$ and different noise levels σ^2 in the range from 10^{-2} to 1 (the direction of increase of σ^2 is indicated by arrows).

the latter regime, corresponding to large values of $\mathcal{E}_0$ and whose lower bound is an increasing function of the noise magnitude, we observe that for sufficiently large $\mathcal{E}_0$ the growth of the quantity $\max_{t\in[0,T]} \mathbb{E}(\mathcal{E}[u^{K,N}(t)])$ in all cases approaches the growth observed in the deterministic case [18].

Since the results presented above show no evidence of the effect of noise on the dependence of the quantities (35) on $\mathcal{E}_0$ when $\mathcal{E}_0$ grows while the noise magnitude stays fixed, to close this section we consider the case in which the noise magnitude is proportional to $\mathcal{E}_0$, i.e.,

$$\sigma^2 = C_\sigma \, \mathcal{E}_0, \tag{36}$$

for a range of different constants C_σ. The quantities (35b) obtained in this way are shown in Figures 10a and 10b. As regards the dependence of the quantity $\max_{t\in[0,T]} \mathcal{E}(\mathbb{E}[u^{K,N}(t)])$ on $\mathcal{E}_0$, in Figure 10a we observe a superlinear growth which is however slower than $\mathcal{E}_0^{3/2}$ characterizing the deterministic case (in fact, from the data it is not entirely obvious if this dependence is strictly in the form of a power law). Concerning the quantity $\max_{t\in[0,T]} \mathbb{E}(\mathcal{E}[u^{K,N}(t)])$, Figure 10b indicates that while for small $\mathcal{E}_0$ it is larger than $\max_{t\geq 0} \mathcal{E}(t)$ obtained in the deterministic case, in the limit of $\mathcal{E}_0 \to \infty$ it reveals the same growth as in the deterministic case, that is, proportional to $\mathcal{E}_0^{3/2}$ with approximately the same constant prefactor.

5 Discussion and Conclusions

The goal of this study was to test whether a stochastic excitation applied to Burgers equation can affect the maximum growth of enstrophy as a function of the initial enstrophy $\mathcal{E}_0$ observed in the deterministic case [18]. In the context of hydrodynamic models based

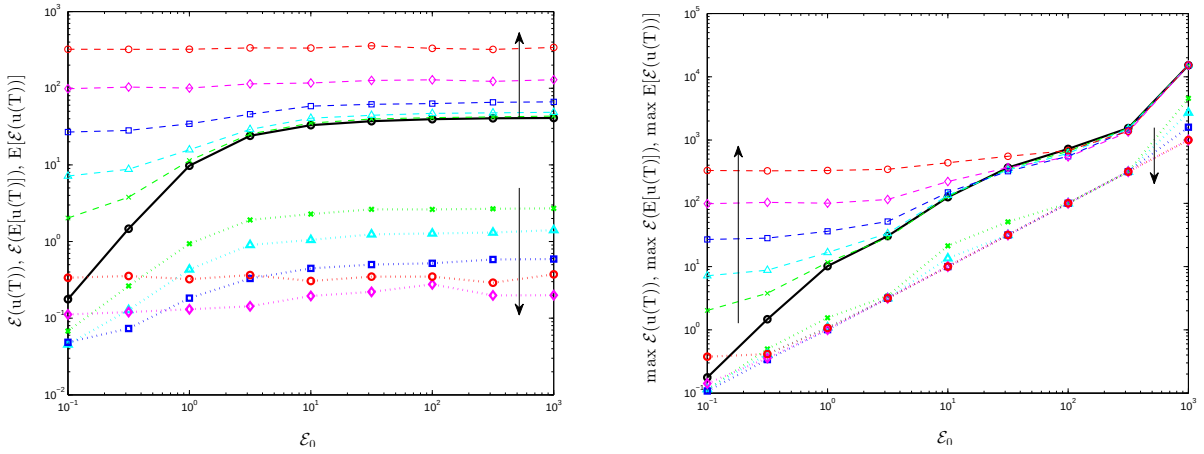

(a) (b)

Figure 7: (a) The values at $t = T = 1.0$ and (b) the maximum values attained in $[0, T]$ of the expected value of the enstrophy $\mathbb{E}(\mathcal{E}[u^{K,N}(t)])$ (dashed lines), the enstrophy of the expected value of the solution $\mathcal{E}(\mathbb{E}[u^{K,N}(t)])$ (dotted lines) and the enstrophy $\mathcal{E}(t)$ of the deterministic solution (thick solid line) as functions of the initial enstrophy $\mathcal{E}_0$ for the initial condition $\tilde{g}_{\mathcal{E}_0,T}$ with $\mathcal{E}_0 = 10$, $T = 1$ and different noise levels σ^2 in the range from 10^{-2} to 1 (the direction of increase of σ^2 is indicated by arrows)

on the Navier-Stokes equation, the enstrophy is a convenient indicator of the regularity of solutions and its growth is inherently related to the problem of finite-time singularity formation [1]. In the stochastic problem considered here, there are two relevant quantities related to the enstrophy, namely, the expected value of the enstrophy $\mathbb{E}(\mathcal{E}[u(t)])$ and the enstrophy of the expected value of the solution $\mathcal{E}(\mathbb{E}[u(t)])$. They are related to each other via Jensen's inequality (32). In the set-up of our problem we allowed for the most "aggressive" form of the stochastic excitation which still ensures that the two quantities are well defined (cf. Section 2). The numerical discretization was carefully designed based on the Monte Carlo sampling.

The effect of the noise was found to depend on the relation between its magnitude σ^2 and the "size" of the initial data as measured by the initial enstrophy $\mathcal{E}_0$. When the noise magnitude is large, the stochastic excitation obscures the intrinsic dynamics and any dependence of the diagnostic quantities (35) on $\mathcal{E}_0$ is lost. Therefore, the relevant regime is when the noise magnitude is "modest" relative to the initial enstrophy $\mathcal{E}_0$, so that the stochastic excitation can be regarded as a "perturbation" of the deterministic dynamics. We observe that the two quantities $\mathbb{E}(\mathcal{E}[u(t)])$ and $\mathcal{E}(\mathbb{E}[u(t)])$ provide, respectively, upper and lower bounds on the enstrophy $\mathcal{E}(t)$ in the deterministic case, cf. (34), with the bounds becoming tighter as the noise magnitude vanishes (Figure 6). The latter case, with the enstrophy of the expected value of the solution $\mathcal{E}(\mathbb{E}[u(t)])$ being lower than the deterministic enstrophy $\mathcal{E}(t)$, can be therefore interpreted in terms of the stochastic excitation having the effect of an increased dissipation of the expected value of the solution. As regards the expected value of the enstrophy, we

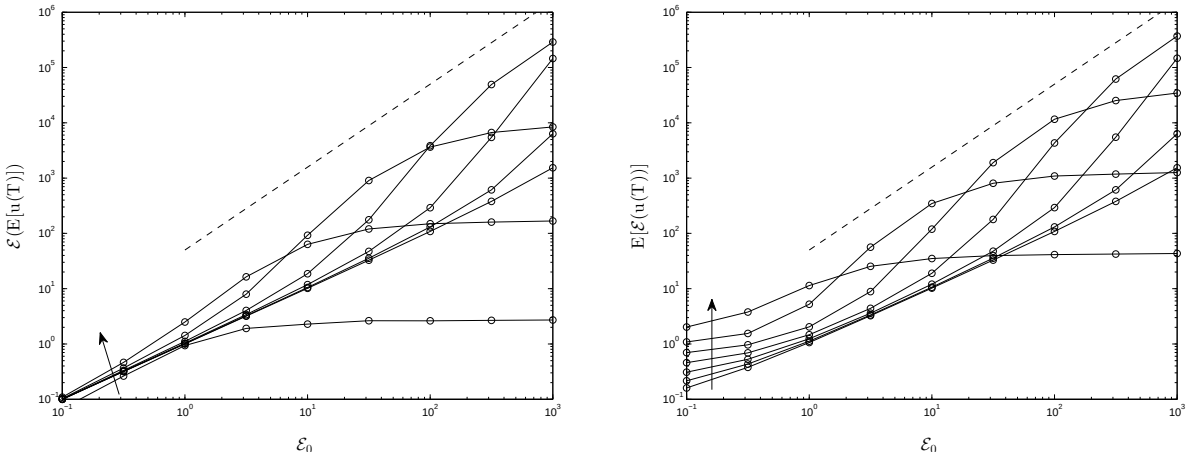

(a) (b)

Figure 8: [Small noise case: $\sigma^2 = 10^{-2}$] Dependence of (a) the enstrophy of the expected value of the solution $\mathcal{E}(\mathbb{E}[u^{K,N}(T)])$ and (b) the expected value of the enstrophy $\mathbb{E}(\mathcal{E}[u^{K,N}(T)])$ on the initial enstrophy $\mathcal{E}_0$ using the initial condition $\tilde{g}_{\mathcal{E}_0,T}$ with T varying from 10^{-3} to 1. Arrows indicate the direction of increasing T and the dashed lines correspond to the power law $C\,\mathcal{E}_0^{3/2}$.

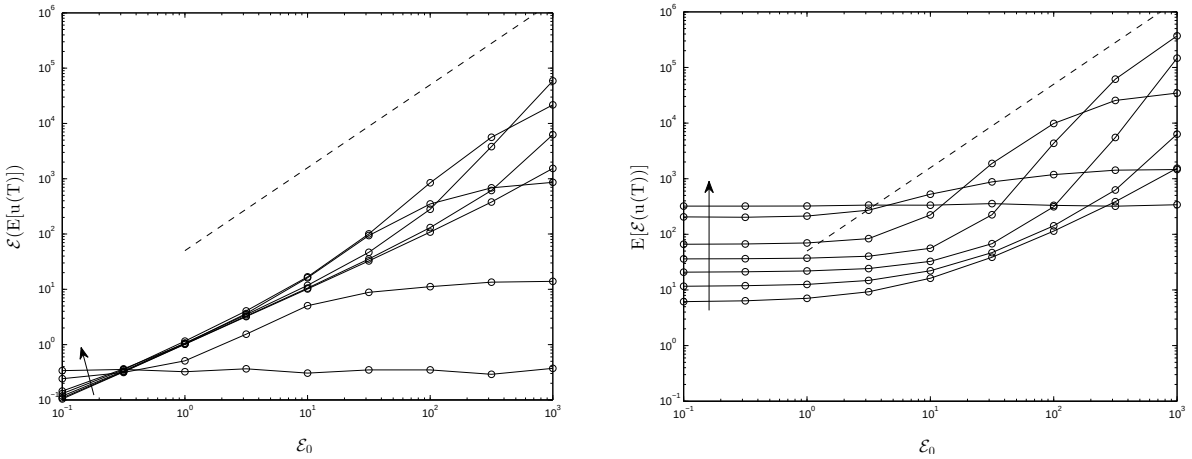

(c) (d)

Figure 9: [Large noise case: $\sigma^2 = 1$] (see previous figure for details).

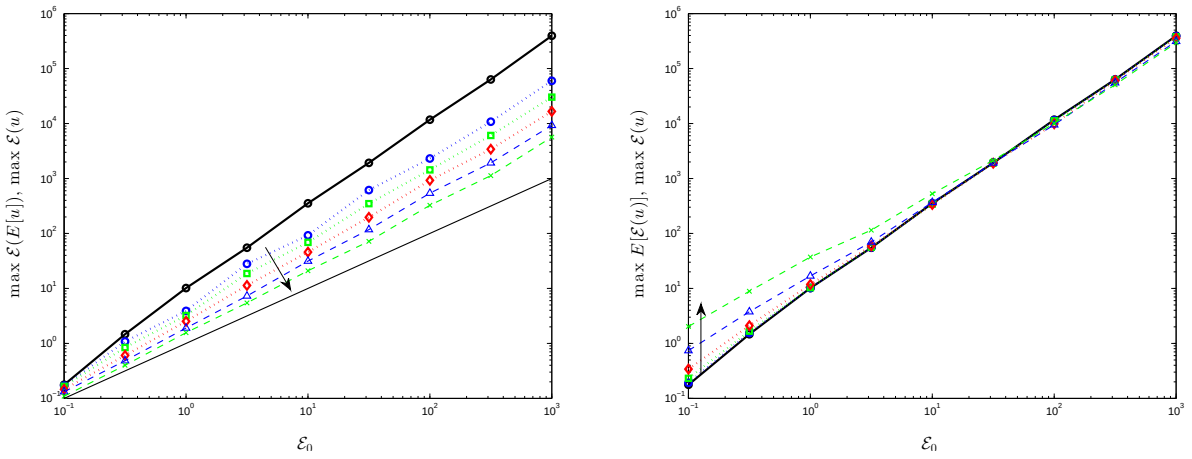

(a) (b)

Figure 10: Dependence of (a) the maximum enstrophy of the expected value of the solution $\max_{t\in[0,T]} \mathcal{E}(\mathbb{E}[u^{K,N}(t)])$ and (b) the maximum expected value of the enstrophy $\max_{t\in[0,T]} \mathbb{E}(\mathcal{E}[u^{K,N}(t)])$ on the initial enstrophy $\mathcal{E}_0$ using the initial conditions $\tilde{g}_{\mathcal{E}_0,T}$ and with noise magnitudes proportional to $\mathcal{E}_0$, cf. (36), with C_σ in the range from 10^{-3} to 10^{-1} (arrow indicate the direction of increase of C_σ). The parameter T is chosen to maximize $\max_{t\in[0,T]} \mathcal{E}(\mathbb{E}[u^{K,N}(t)])$ in (a) and $\max_{t\in[0,T]} \mathbb{E}(\mathcal{E}[u^{K,N}(t)])$ in (b). The thick black solid line corresponds to the quantity $\max_{t\in[0,T]} \mathcal{E}(t)$ obtained in the deterministic case, whereas the thin black solid line in (a) represents the power law $\mathcal{E}_0^1$.

observed in Figure 10a that in the limit $\mathcal{E}_0 \to \infty$ the quantity $\max_{t\geq 0} \mathbb{E}(\mathcal{E}[u(t)])$ exhibits the same dependence on $\mathcal{E}_0$ as in the deterministic case, i.e., it remains proportional to $\mathcal{E}_0^{3/2}$, even for the noise magnitude increasing proportionally to $\mathcal{E}_0$. Thus, this demonstrates that the stochastic excitation *does not* amplify the maximum growth of enstrophy as a function of the initial enstrophy $\mathcal{E}_0$.

A number of related questions remain open. First of all, in the present study we numerically solved the stochastic Burgers equation (1) using the extreme initial data $\tilde{g}_{\mathcal{E}_0,T}$ which was found in [18] by solving a deterministic variational optimization problem. It is however possible that by solving a corresponding *stochastic* optimization problem one might obtain initial data g leading to an even larger growth of enstrophy in finite time. While such problems are harder to solve than the deterministic one, they are in principle amenable to solution using stochastic programming methods [32]. In a similar spirit, it is equally interesting to obtain *rigorous* estimates on $d\mathcal{E}/dt$ and $\max_{t\geq 0} \mathcal{E}(t)$ in the stochastic setting in terms of $\mathcal{E}_0$ and the properties of noise, thereby generalizing the bounds available for the deterministic case [21, 18]. Similar questions concerning the interplay between the stochastic excitation and extreme behavior, including possible singularity formation, also arise in the context of the two-dimensional and three-dimensional Navier-Stokes and Euler equations. Addressing at least some of these issues is one of the goals of the ongoing research program mentioned in Introduction.

Acknowledgements

The authors would like to thank Dr. Diego Ayala for his help with computing the optimal initial data $\tilde{g}_{\mathcal{E}_0,T}$ [18]. This research was supported by NSERC (Canada) and FCT Doctoral Grant (Portugal).

A White Noise and Well–Posedness of Enstrophy

In this appendix we provide a justification why Gaussian white noise does not yield a solution of system (1) with well-defined enstrophy and is thus not applicable to our problem. Suppose u is a mild solution satisfying equation (9), which we restate here for convenience,

$$u(t) = e^{tA}g - \frac{1}{2}\int_0^t e^{(t-s)A}\partial_x u^2\, ds + \sigma \int_0^t e^{(t-s)A}\, dW(s), \tag{9'}$$

with an infinite-variance noise W. We now study each of the terms appearing on the right-hand side of (9).

Analysis of the first term: under the assumption that $g \in L^2_p$, so that $\sum_{k\in\mathbb{Z}} |\hat{g}_k|^2 < \infty$, we have that $e^{tA}g \in H^1_p$ (actually H^ℓ_p for any $\ell \geq 0$), since

$$\|e^{tA}g\|^2_{H^1_p} = \sum_{k\in\mathbb{Z}} \frac{1+4\pi^2k^2}{e^{4\nu\pi^2k^2t}}|\hat{g}_k|^2 < \infty$$

which is true because the exponentials dominate all other factors.

Analysis of the second term: under the assumption that $u \in L^2(\Omega, C([0,T], L^4_p))$, so that $u^2 \in L^2(\Omega, C([0,T], L^2_p))$, we can write

$$u^2 = \sum_{k\in\mathbb{Z}} \hat{y}_k \phi_k \quad \text{with} \quad \sum_{k\in\mathbb{Z}} \|\hat{y}_k\|^2_{L^2(\Omega, C([0,T],\mathbb{C}))} = \sum_{k\in\mathbb{Z}} \mathbb{E}\left[\sup_{0\le t\le T} |\hat{y}_k|^2\right] < \infty,$$

so that

$$\partial_x u^2 = 2\pi i \sum_{k\in\mathbb{Z}} k \hat{y}_k \phi_k$$

and

$$\int_0^t \frac{1}{2} e^{(t-s)A} \partial_x u^2 \, ds = \sum_{k\in\mathbb{Z}} \left[\int_0^t \frac{1}{2} 2\pi i k e^{-4\nu\pi^2 k^2 (t-s)} \hat{y}_k(s)\, ds\right] \phi_k;$$

now each of the coefficients in the sum above can be bounded as

$$\begin{aligned}\left|\int_0^t \frac{1}{2} 2\pi i k e^{-4\nu\pi^2 k^2 (t-s)} \hat{y}_k(s)\, ds\right| &\le \int_0^t \pi k e^{-4\nu\pi^2 k^2 (t-s)} ds \sup_{0\le t\le T} |\hat{y}_k| \\ &= \frac{1}{\nu\pi k}\left(1 - e^{-8\nu\pi^2 k^2 t}\right) \sup_{0\le t\le T} |\hat{y}_k| \le \frac{1}{\nu\pi k} \sup_{0\le t\le T} |\hat{y}_k|,\end{aligned}$$

so that the second term in (9) is also in H^1_p with

$$\begin{aligned}\left\|\int_0^t \frac{1}{2} e^{(t-s)A} \partial_x u^2 \, ds\right\|^2_{L^2(\Omega, H^1_p)} &\le \sum_{k\in\mathbb{Z}} (1 + 4\pi^2 k^2) \left\|\frac{1}{\nu\pi k} \sup_{0\le t\le T} |\hat{y}_k|\right\|^2_{L^2(\Omega,\mathbb{C})} \\ &= \sum_{k\in\mathbb{Z}} \frac{1 + 4\pi^2 k^2}{\nu^2 \pi^2 k^2} \|\hat{y}_k\|^2_{L^2(\Omega, C([0,T],\mathbb{C}))} < \infty\end{aligned}$$

which follows from the summability of $\|\hat{y}_k\|^2$.

Analysis of the third term: writing it in terms of a Fourier series

$$\sigma \int_0^t e^{(t-s)A}\, dW(s) = \sum_{k\in\mathbb{Z}} \hat{W}_k(t)\, \phi_k,$$

we obtain (for $k > 0$ with the cases $k = 0$ and $k < 0$ handled similarly)

$$\hat{W}_k(t) = \sigma \int_0^t e^{-4\nu\pi^2 k^2 (t-s)} \left(\frac{\sqrt{2}}{2} d\beta_{2k}(s) - i \frac{\sqrt{2}}{2} d\beta_{2k}(s)\right)$$

which is a random variable with the second moment given by

$$\|\hat{W}_k(t)\|^2_{L^2(\Omega,\mathbb{C})} = \sigma^2 \int_0^t e^{-8\nu\pi^2 k^2 (t-s)}\, ds = \frac{\sigma^2}{8\nu\pi^2 k^2}\left(1 - e^{-8\nu\pi^2 k^2 t}\right);$$

from this we see that the third term is in L^2 but not in H^1_p, as for any $t > 0$ we have

$$\left\| \sigma \int_0^t e^{(t-s)A}\, dW(s) \right\|^2_{L^2(\Omega, H^1_p)} = \sum_{k\in\mathbb{Z}} (1+4\pi^2 k^2) \|\hat{W}_k\|^2_{L^2(\Omega,\mathbb{C})} = \frac{\sigma^2}{8\nu\pi^2} \sum_{k\in\mathbb{Z}} \frac{1+4\pi^2k^2}{k^2} (1-e^{-8\nu\pi^2k^2t}) = \infty.$$

So, we conclude that while the first two terms on the right-hand side of (9) are in H^1_p (and hence also in L^2), the third one is only in L^2 and not in H^1_p. Thus, for any $t > 0$ $u(t)$, being the left-hand side of (9), is in L^2 but not in H^1_p, and consequently the enstrophy obtained with Gaussian white noise is not well defined.

B Proof of Lemma 6

Proof. (To simplify the notation here z^* denotes the complex conjugate of z)

$$\begin{aligned}
\left\| \mathbb{E}\left[u_n^{K,N}\right] - u_n^{K,N,S} \right\|^2_{L^2(\Omega,H^1_p)} &= \int_\Omega \left\| \mathbb{E}\left[u_n^{K,N}\right] - u_n^{K,N,S} \right\|^2_{H^1_p} d\mathbb{P}(\omega) \\
&= \int_\Omega \sum_{k\in\mathbb{Z}} (1+4\pi^2k^2) \left| \mathbb{E}\left[\hat{u}_{k,n}^{K,N}\right] - \hat{u}_{k,n}^{K,N,S} \right|^2 d\mathbb{P}(\omega) \\
&= \sum_{k\in\mathbb{Z}} (1+4\pi^2k^2) \int_\Omega \left| \mathbb{E}\left[\hat{u}_{k,n}^{K,N}\right] - \frac{1}{S}\sum_{s=1}^S \hat{u}_{k,n,s}^{K,N,S} \right|^2 d\mathbb{P}(\omega) \\
&= \sum_{k\in\mathbb{Z}} (1+4\pi^2k^2) \int_\Omega \left| \mathbb{E}\left[\hat{u}_{k,n}^{K,N}\right] \right|^2 - \mathbb{E}\left[\hat{u}_{k,n}^{K,N}\right] \left(\frac{1}{S}\sum_{s=1}^S \hat{u}_{k,n,s}^{K,N,S} \right)^* \\
&\qquad - \left(\mathbb{E}\left[\hat{u}_{k,n}^{K,N}\right] \right)^* \frac{1}{S}\sum_{s=1}^S \hat{u}_{k,n,s}^{K,N,S} + \left| \frac{1}{S}\sum_{s=1}^S \hat{u}_{k,n,s}^{K,N,S} \right|^2 d\mathbb{P}(\omega) \\
&= \sum_{k\in\mathbb{Z}} (1+4\pi^2k^2) \Bigg(\left| \mathbb{E}\left[\hat{u}_{k,n}^{K,N}\right] \right|^2 - \mathbb{E}\left[\hat{u}_{k,n}^{K,N}\right] \left(\mathbb{E}\left[\hat{u}_{k,n}^{K,N}\right] \right)^* \\
&\qquad - \left(\mathbb{E}\left[\hat{u}_{k,n}^{K,N}\right] \right)^* \mathbb{E}\left[\hat{u}_{k,n}^{K,N}\right] + \int_\Omega \frac{1}{S^2} \sum_{s,s'=1}^S \hat{u}_{k,n,s}^{K,N,S} \left(\hat{u}_{k,n,s'}^{K,N,S} \right)^* d\mathbb{P}(\omega) \Bigg) \\
&= \sum_{k\in\mathbb{Z}} (1+4\pi^2k^2) \left(- \left| \mathbb{E}\left[\hat{u}_{k,n}^{K,N}\right] \right|^2 + \frac{S}{S^2} \mathbb{E}\left[\left| \hat{u}_{k,n}^{K,N} \right|^2 \right] + \frac{S^2-S}{S^2} \left| \mathbb{E}\left[\hat{u}_{k,n}^{K,N}\right] \right|^2 \right) \\
&= \sum_{k\in\mathbb{Z}} (1+4\pi^2k^2) \frac{1}{S} \left(\mathbb{E}\left[\left| \hat{u}_{k,n}^{K,N} \right|^2 \right] - \left| \mathbb{E}\left[\hat{u}_{k,n}^{K,N}\right] \right|^2 \right) \\
&= \sum_{k\in\mathbb{Z}} (1+4\pi^2k^2) \frac{1}{S} \mathbb{E}\left[\left| \hat{u}_{k,n}^{K,N} - \mathbb{E}\left[\hat{u}_{k,n}^{K,N}\right] \right|^2 \right] \\
&= \frac{1}{S} \left\| u_n^{K,N} - \mathbb{E}\left[u_n^{K,N}\right] \right\|^2_{L^2(\Omega,H^1_p)}.
\end{aligned}$$

□

References

[1] C. R. Doering. The 3D Navier-Stokes problem. *Annual Review of Fluid Mechanics*, pages 109–128, 2009.

[2] C. L. Fefferman. Existence and smoothness of the Navier-Stokes equation. available at `http://www.claymath.org/millennium/Navier-Stokes_Equations/navierstokes.pdf`, 2000. Clay Millennium Prize Problem Description.

[3] J. D. Gibbon, M. Bustamante, and R. M. Kerr. The three–dimensional Euler equations: singular or non–singular? *Nonlinearity*, 21:123–129, 2008.

[4] Franco Flandoli. *Random Perturbation of PDEs and Fluid Dynamic Models*. Lecture Notes in Mathematics. Springer, 2015.

[5] J. Kim and T.R. Bewley. A linear systems approach to flow control. *Ann. Rev. Fluid Mech.*, 39:383–417, 2007.

[6] R. A. Adams and J. F. Fournier. *Sobolev Spaces*. Elsevier, 2005.

[7] A. Debussche and L. Di Menza. Numerical simulation of focusing stochastic nonlinear Schrödinger equations. *Physica D*, 162:131–154, 2002.

[8] Martin Hairer. Solving the KPZ equation. *Annals of Mathematics*, 178:559–664, 2014.

[9] L. Bertini, N Cancrini, and G Jona-Lasinio. The stochastic Burgers equation. *Communications in Mathematical Physics*, 165:211–232, 1994.

[10] István Gyöngy and David Nualart. On the stochastic Burgers' equation in the real line. *The Annals of Probability*, 27:782–802, 1999.

[11] G. Da Prato, A. Debussche, and R. Temam. Stochastic Burgers' equation. *Nonlinear Differential Equations and Applications*, 1:289–402, 1994.

[12] István Gyöngy. Existence and uniqueness results for semilinear stochastic partial differential equations. *Stochastic Processes and their Applications*, 73:271–299, 1998.

[13] Aureli Alabert and István Gyöngy. On numerical approximation of stochastic Burgers' equation. In *From stochastic calculus to mathematical finance*, pages 1–15. Springer, 2006.

[14] D. Blomker and A. Jentzen. Galerkin approximations for the stochastic Burgers equation. *SIAM Journal on Numerical Analysis*, 51:694–715, 2013.

[15] M. Hairer and K. Matetski. Optimal rate of convergence for stochastic Burgers-type equations. arXiv:1504:05134, 2015.

[16] H. Kreiss and J. Lorenz. *Initial-Boundary Value Problems and the Navier-Stokes Equations*, volume 47 of *Classics in Applied Mathematics*. SIAM, 2004.

[17] Christian Klein and Jean-Claude Saut. A numerical approach to blow-up issues for dispersive perturbations of Burgers' equation. *Physica D*, 295–296:46–65, 2015.

[18] D. Ayala and B. Protas. On maximum enstrophy growth in a hydrodynamic system. *Physica D*, 240:1553–1563, 2011.

[19] D. Ayala and B. Protas. Maximum palinstrophy growth in 2D incompressible flows. *Journal of Fluid Mechanics*, 742:340–367, 2014.

[20] D. Ayala and B. Protas. Vortices, maximum growth and the problem of finite-time singularity formation. *Fluid Dynamics Research*, 46(3):031404, 2014.

[21] L. Lu and C. R. Doering. Limits on enstrophy growth for solutions of the three-dimensional Navier–Stokes equations. *Indiana University Mathematics Journal*, 57:2693–2727, 2008.

[22] Sergei Kuksin and Armen Shirikyan. *Mathematics of two-dimensional turbulence*. Cambridge University Press, 2012.

[23] J. F. Bonder and P. Groisman. Timespace white noise eliminates global solutions in reaction-diffusion equationse. *Physica D*, 238:2009–215, 2009.

[24] M. Dozzi, E. T. Kolkovska, and J.A. Lopez-Mimbela. *Modern Stochastics and Applications*, chapter Finite-time blowup and existence of global positive solutions of a semi-linear SPDE with fractional noise, pages 95–108. Springer Optimization and Applications. Springer, 2013.

[25] Yan Zeng. *Blow-up Results for Stochastic Heat Equations*. PhD thesis, University of Rochester, 2013.

[26] M. Röckner, R. Zhu, and X. Zhu. Local existence and non-explosion of solutions for stochastic fractional partial differential equations driven by multiplicative noise. *Stochastic Processes and their Applications*, 124:1974–2002, 2014.

[27] Martin Hairer. Singular stochastic PDEs. In *Proceedings of the ICM*, 2014.

[28] Gabriel J. Lord, Catherine E. Powell, and Tony Shardlow. *An Introduction to Computational Stochastic PDEs*. Cambridge University Press, 2014.

[29] C. Canuto, A. Quarteroni, Y. Hussaini, and T. A. Zang. *Spectral Methods*. Scientific Computation. Springer, 2006.

[30] D. Pelinovsky. Sharp bounds on enstrophy growth in the viscous Burgers equation. *Proceedings of Royal Society A*, 468:3636–3648, 2012.

[31] D. Pelinovsky. Enstrophy growth in the viscous Burgers equation. *Dynamics of Partial Differential Equations*, 9:305–340, 2012.

[32] A. Ruszczyński. *Nonlinear Optimization*. Princeton University Press, 2006.